Title: Carbon dioxide efflux and ecosystem metabolism of small forest lakes

Authors: Kenneth Thorø Martinsen[1], Theis Kragh[1], Kaj Sand-Jensen[1]

[1]Freshwater Biological Laboratory, Biological Institute, University of Copenhagen, Universitetsparken 4, 3rd floor, 2100 Copenhagen, Denmark

Corresponding author: Kenneth Thorø Martinsen, +45 60709007, kenneth2810@gmail.com

Keywords: small lakes, forest lakes, carbon dioxide flux, oxygen flux, net ecosystem production, gas exchange velocity

Acknowledgments: We are thankful for grant support from COWIfonden and the Carlsberg Foundation (CF14-0136) donated to Kaj Sand-Jensen towards the study of CO_2 fluxes and carbon dynamics in small lakes. We thank Sara Schousboe for proofreading. We thank the two anonymous reviewers for their constructive comments which helped improve the manuscript.

ORCID:

Kenneth Thorø Martinsen 0000-0001-8064-513X

Theis Kragh 0000-0002-9760-2571

Kaj Sand-Jensen 0000-0003-2534-4638

Abstract

Small lakes are numerous in the landscape and closely connected to the terrestrial environment, which strongly influences the system scale carbon cycling. However, despite their importance in large-scale carbon budgets, small lakes remain understudied compared to large lakes. We investigated oxygen and carbon dynamics in four small Danish forest lakes over a year. Continuous pH measurements were used to establish a high-frequency time series of CO_2 partial pressure and 1169 direct measurements of air-water CO_2 flux were performed using floating chambers. Net ecosystem oxygen production (NEP) was derived from free-water oxygen measurements in order to quantify the contribution of in-lake aerobic metabolism to the air-water CO_2 flux. We found that the forest lakes, on average, were 10-fold CO_2 supersaturated. The two most intensively studied lakes had mean CO_2 effluxes of 36.3 mol m^{-2} $year^{-1}$. The CO_2 effluxes exceeded NEP during all months implying that the CO_2 generated by aerobic respiration alone could not account for the observed CO_2 efflux. The observed discrepancy is likely promoted by a hydrologic CO_2 input and/or anaerobic sediment processes generating CO_2 without a concurrent consumption of O_2. A broad-scale national analysis showed that the CO_2 efflux increased as lake size decreased despite lower gas exchange velocity. Small lakes also showed higher excess CO_2 efflux compared to O_2 influx. Overall, small lakes and forest lakes in particular have high CO_2 effluxes and high CO_2 supersaturation. However, the contribution of hydrological inputs and anaerobic sediment processes to the net CO_2 efflux remains elusive.

Introduction

Small inland water bodies have recently received increasing attention in global carbon budgets due to their widespread occurrence, high combined surface area and high concentrations of dissolved greenhouse gases (carbon dioxide (CO_2) and methane (CH_4); Downing et al. (2006); Holgerson and Raymond (2016)). The tight connection to the terrestrial environment and high input of allochthonous organic carbon promote heterotrophic activity in the small water bodies with bacterial and eucaryote respiration exceeding primary production (Sand-Jensen and Staehr 2007; Staehr et al. 2012). Net heterotrophic dominance may be particularly pronounced in small forest lakes where external organic input is high and primary production is reduced by light-absorbing humic substances and shading from surrounding trees (Holgerson 2015; Weyhenmeyer et al. 2015).

Dissolved CO_2 and CH_4 derived from heterotrophic metabolism in the lakes and the terrestrial surroundings connected via water input are usually supersaturated relative to the atmosphere (Kling et al. 1991; Cole et al. 1994). The CO_2 transport across the air-water interface is determined by the concentration gradient times the gas exchange velocity (MacIntyre et al. 1995). The gas exchange velocity is driven by the near-surface turbulence (Vachon et al. 2010), which can be partitioned into turbulence generated by wind-shear or convection (Imberger 1985). Heating of surface waters by incoming solar radiation stabilizes the water column and dampens turbulence, while wind-shear and convection (heat loss) deepen the mixed layer and generate turbulence (Read et al. 2012). Large diel variability in surface water temperature has been observed in small lakes, which indicates that convective mixing may be important for surface water turbulence (Woolway et al. 2016; Martinsen et al. 2019). However, previous studies in very small lakes (<1000 m^2) find wind speed to be a significant predictor of gas exchange velocity (Holgerson et al. 2017; Kragh et al. 2017).

The gas transfer velocity can be quantified by measuring the concentration gradient and gas flux (Cole et al. 2010). Several empirical relationships between gas exchange velocity and wind speed have been established for lakes (Cole and Caraco 1998; Crusius and Wanninkhof 2003) along with complex surface-renewal models, which include the contribution by convection (Read et al. 2012). Gas exchange velocity is expected to increase with lake surface area due to stronger influence of winds and waves (Vachon and Prairie 2013). However, only few measurements are from small lakes (<0.01 km^2) and the relative influence of the drivers remains difficult to resolve (Holgerson et al. 2017). Other factors such as extensive sheltering and emergent vegetation may further complicate attempts to model gas exchange velocities in small lakes. In order to reduce the uncertainty associated with estimation of ecosystem metabolism and considerations of gas flux from long-term concentration measurements, model improvements for small lakes are needed (Dugan et al. 2016).

While a portion of the CO_2 emitted from lake surfaces is derived from internal metabolism, another, often unknown, portion is derived from terrestrial watershed processes (Striegl and Michmerhuizen 1998; Maberly et al. 2013). In streams and rivers, the influence of internal CO_2 formation increases relative to the external input as streams become larger (Hotchkiss et al. 2015). The external input is in the form of dissolved and particulate organic matter along with dissolved CO_2, which arises from soil respiration and chemical weathering in the watershed (Wilkinson et al. 2013; Marcé et al. 2015). Thus, hydrology may be very influential on lake processes as carbon is received by ground- and surface water flows, which can increase lake CO_2 partial pressure and atmospheric evasion (Marotta et al. 2011).

The contribution of internal and external sources to CO_2 emission from water bodies can be examined by carbon mass-balance models (Finlay et al. 2010) or by the stoichiometric relationship between CO_2 and O_2 lake-atmosphere fluxes (Torgersen and Branco 2008). A molar ratio between CO_2 efflux and O_2 influx close to 1.0 suggests that emissions are driven entirely by internal aerobic metabolism. The relationship between internal processes and external input becomes more obvious when net ecosystem production (NEP) is used instead of O_2 flux. NEP is a direct measure of the current daily metabolic balance independent of day-to-day differences in gas exchange velocity and carry-over of CO_2 from previous days input and metabolic balance. NEP is the difference between gross primary production (GPP) and respiration (R) and constrains the amount of CO_2 generated by internal aerobic metabolism, which later can be emitted to the atmosphere. For example, McDonald et al. (2013) observed a significant proportion of net autotrophic lakes with positive NEP, i.e. net O_2 efflux and CO_2 sink in ecosystem metabolism. Nonetheless, there was a net CO_2 efflux suggesting a role of externally derived CO_2. However, generation of CO_2 without consumption of O_2 may also take place by anaerobic processes such as fermentation and denitrification (Torgersen and Branco 2007). These processes remain difficult to quantify, but were found to have minor influence compared with the contribution of aerobic metabolism in three small lakes (Wilkinson et al. 2016). Anaerobic organic matter degradation below the sediment surface with sulfate, manganese or oxidized iron as electron acceptors usually results in a 1:1 relationship between CO_2 formation and O_2 consumption because the reduced form of S, Mn and Fe formed are re-oxidized at the aerobic sediment surface (Torgersen and Branco 2008). In contrast, N_2 and N_2O formed along with CO_2 by denitrification are not re-oxidized in the lake. The same is true when sulfate and iron oxides are received from outside, oxidize organic matter to CO_2 and become buried in the sediments as iron sulfides (Sørensen et al. 1979). Likewise, for methane produced by fermentation, which may exit the system by ebullition or transport mediated through air lacunae of floating-leaves or emergent plants; those pathways are likely important in small lakes and are not causing methane re-oxidation (Bastviken et al. 2004).

Our overall objective was to quantify CO_2 emission to the atmosphere and whole-system metabolism in four small forest lakes. We measured these processes directly and, when possible, over a full year to account for seasonal variations.. In order to put measurements on small forest lakes into a broader perspective, we compared them with a national analysis of the relationship between CO_2 and O_2 air-water gas exchange across multiple lake size classes. Specifically, we hypothesized that: 1) small forest lakes would be CO_2 net sources to the atmosphere throughout the year due to the high input of degradable organic matter and free CO_2 in the water received from the terrestrial environment, 2) existing wind models of gas exchange velocity would perform poorly in small sheltered lakes because of local conditions, 3) though gas exchange velocity is lower compared to larger lakes, high CO_2 emissions from small lakes may, nonetheless, be sustained by internal heterotrophy and external input of organic matter and CO_2.

Methods

Study area

We measured a wide range of environmental variables in four small forest lakes during different seasons and meteorological conditions from summer 2017 to summer 2018 (Table 1). The lakes are located in Grib Forest (Gribskov), Zealand, Denmark, which consists of mixed deciduous and coniferous trees with scattered small lakes and wetland areas (Fig. 1). Lakes are named A to D from north to south on the map. The lakes are typical small, shallow forest lakes with a natural hydrological regime. Lake B receives water from Lake A during periods of high-water table. Lakes B and C have intermittent surface outflows and are not connected. Lake D does not have any surface in- or outflows. Sampling was initiated in the four lakes in August 2017 and finished in October 2017 in Lake A (12.272718 °N, 55.986350 °E) and Lake D (12.271635 °N, 55.960441 °E) and finished in June 2018 in Lake B (12.271820 °N, 55.985858 °E) and Lake C (12.269975 °N, 55.984428 °E) after almost a year.

A meteorological station (HOBO Onset Computers, Bourne, MA, USA), which measured air temperature (HOBO U23 Pro v2), wind speed (HOBO S-WSET-A), incident irradiance (PAR; HOBO S-LIA-M003) and relative humidity (HOBO U23 Pro v2) was placed 2.5 m above the ground in an open landscape close to Lake D. From spring 2018, atmospheric pressure was also measured (HOBO U-20-001-04) and when unavailable, we used the daily atmospheric pressure for the region (DMI 2017).

Lake variables

In the lakes, we measured water temperature and light intensity profiles (five sensors, HOBO UA-002-64, accuracy of ± 0.53 °C), oxygen (two sensors, MiniDOT, PME, Vista, CA, USA) and pH (one sensor, pHTemp2000 MadgeTech data logger with an Omega pH electrode). Sensors were mounted on steel pegs pushed into the sediment. The oxygen sensors were calibrated at 0% (water aerated with N_2) and 100% saturation, while pH sensors were calibrated at pH 4 and 7. Oxygen and pH sensors were calibrated before and after each deployment and corrected for drift (if any), assumed to be linear over time. Periodically, wind speed (HOBO S-WSET-A) was measured 0.3-0.5 m above the water surface at the location of submerged sensors in all four lakes. Wind speed above the lake surface was compared to simultaneous measurements at the permanent meteorological station in order to establish a relationship between local wind speed for each lake and wind speed at the meteorological station as well as enable continuous wind speed estimates for each lake (Fig. S1). Surface water samples were collected and analyzed the following day for alkalinity (acid-neutralizing capacity) by acidimetric titration (Gran 1952), chlorophyll *a* of filtered particles extracted in ethanol (Jespersen and Christoffersen 1987), and colored dissolved organic matter (CDOM) as spectrophotometric absorption at 440 nm of a 0.07 µm (GF/F) filtrate (Sand-Jensen and Staehr 2007). Frozen water samples were thawed and analyzed for nutrients (total-P, total-N, ortho-phosphate, nitrate and ammonium) on an auto analyzer (AA3HRAutoAnalyzer, SEAL, WI, USA) using standard protocols (University of Copenhagen 1992). Daily water column light attenuation (k_z) was calculated from the vertical light intensity measurements (Andersen et al. 2017). During high-water table in spring 2018, bathymetric maps were made by measuring depth at regular intervals (0.5–1.0 m) along three to four transects across each lake with concurrent delineation of the lake by a handheld GPS followed by estimation of surface area. To establish relationships between surface area as a function of water depth, we fitted smoothing splines to calculations of the area represented by each depth interval. Integrating this function yields lake volume as a function of depth. Depth was measured manually at every visit.

Carbon dioxide gas flux

We used manual floating chambers very similar to the one described by Bastviken et al. (2015) to measure both CO_2 partial pressure and water-air CO_2 flux. We used floating chambers of two sizes: surface areas = 0.08/0.03 m^2 and air volumes = 0.0075/0.0056 m^3. The large and small sizes were used for flux measurements while only the large size was used for partial pressure measurements. We also used a floating chamber of the large type modified to perform automatic gas flux measurements by renewing the head space using an air pump and timer as described by Martinsen et al. (2018). The chambers were equipped with CO_2 mini-loggers (CO_2 ELG module, Senseair, Sweden) and a battery supply (9V) inside an inverted plastic dome equipped with a floating collar. The headspace CO_2 partial pressure was logged at 2-5 minute intervals for flux measurements and 10-15 minute intervals for partial pressure equilibration. Manual measurements of CO_2 flux lasted 20-60 minutes. The CO_2 mini-loggers were frequently calibrated in CO_2 free air (N_2) following the manufacturers' guidelines. The automatic chambers were deployed on several occasions with sampling cycles of approximately 30 minutes or, on one occasion 60 minutes during winter, followed by 5-10 minutes' evacuation of the chamber head space. The flux (F, reported as mmol m^{-2} day^{-1}) was calculated from the linear change in headspace CO_2 mixing ratio (ppm) as:

$$F=\frac{dCO_2}{dt}\frac{P_{amb}V}{RTA}F=\frac{dCO_2}{dt}\frac{P_{amb}V}{RTA} \qquad \text{(Eq. 1)}$$

The first term is the increase of CO_2 partial pressure over time calculated by linear regression, V is the chamber volume (m^3), R is the universal gas constant (m^3 atm K^{-1} mol^{-1}), P_{amb} is the ambient atmospheric pressure (atm), T is the ambient temperature (K) and A is the chamber area in contact with the lake surface (m^2). The CO_2 partial pressure in the chambers usually followed a linear time course. When the r-square value of the linear regression was below 0.9, the measurement was discarded (Guérin et al. 2007).

Carbon dioxide partial pressure and gas exchange velocity

Measured pH, water temperature and linearly interpolated alkalinity, enabled calculation of a high frequency time series of CO_2 partial pressure in surface waters (Weyhenmeyer et al. 2012). Moreover, floating chambers were left to equilibrate to obtain the surface water CO_2 partial pressure as described by Natchimuthu et al. (2017). Floating chamber measurements allowed estimates of water CO_2 partial pressure to be constrained and to evaluate the validity of the pH-alkalinity method to calculate CO_2. However, as the measurement time scales differ, we do not expect to obtain closely similar estimates from the two methods.

In Lake A, pH and alkalinity were generally lower and CDOM higher than in the other three lakes (Table 1). This resulted in unrealistically high CO_2 values, which is in accordance with previous results from the same habitat type (Abril et al. 2015). Only the manually measured CO_2 flux from Lake A was used in further analysis.

The gas flux (F) across the air-water interface can be expressed as the product of the gas exchange velocity (k, m day^{-1}) and the difference between the actual and saturation gas concentration (C_{water} and C_{sat}, mg L^{-1}):

$$F=k\left(C_{water}-C_{sat}\right) \qquad \text{(Eq. 2)}$$

Knowing both F and the difference in CO_2 partial pressure, the gas exchange velocity (k) can be calculated normalizing to a Schmidt number of 600 (k_{600}, Jähne et al. (1987)) according to the temperature specific Schmidt number of the particular gas (Wanninkhof 1992). The atmospheric CO_2 partial pressure was measured using the same mini-loggers placed 0.25-1 m above the lake surfaces on several occasions. We used the mean value of all these 5164 measurements (516 µatm, SD = 96.5 µatm) in further calculations of CO_2 partial pressure gradient between water and atmosphere. Because CO_2 partial pressure was extensively supersaturated in the lake water, the small supersaturation in the air above lake surfaces was not essential for the calculations.

We established relationships between k_{600} and the wind speed adjusted to each site. The adjustment of wind speed was done by fitting a linear model between the wind speed measured just above the water surface at each site (response) and wind speed at the meteorological station (predictor). When site measurements were available they were used, while gaps were filled by predictions from the linear wind model. Wind speeds were standardized to 10 m height above ground before comparison (Winslow et al. 2016). We compared our k_{600} values to four previously published models using the site adjusted wind speed, water temperature and meteorological variables as input to dedicated functions in the *LakeMetabolizer* package (Winslow et al. 2016). Two wind speed models (Cole and Caraco 1998; Crusius and Wanninkhof 2003), a surface renewal model (Read et al. 2012) and a boundary layer model, which includes wind shear and buoyancy flux (Heiskanen et al. 2014), were examined.

Ecosystem metabolism

Ecosystem metabolism was calculated from measurements of oxygen, water temperature and light intensity for each day using an inverse modeling approach as described by Solomon et al. (2013). The diel oxygen cycle is assumed to be the result of three processes: Gross primary production (GPP), respiration (R) and atmospheric gas exchange (F):

$$\frac{dO_2}{dt} = GPP - R + F = \alpha * I - r_{20} * 1.073^{(T-20)} + -k * d * (C_{water} - C_{sat}) / z_{mix} \qquad \text{(Eq. 3)}$$

Gross primary production (GPP) was parameterized using a linear relationship with light intensity (I, Hanson et al. (2003)) and respiration (R) as temperature (T) dependent with a Q_{10} of 2 (Jørgensen and Bendoricchio 2001). The free parameters α and r_{20} were estimated using maximum likelihood methods; Martinsen et al. (2017) offer a detailed description of the parameter estimation procedure. The thermocline depth (z_{max}) was calculated according to *rLakeAnalyzer* (Read et al. 2011). The parameter d is a dummy variable coded as 0 or 1 depending on whether z_{max} was shallower or deeper, respectively, than the position of oxygen sensors in the water column. On days with ice cover, d was set to 0. In Lake A, metabolism could not be estimated reliably, which was likely due to a larger influence of physical processes relative to metabolic processes on the diel dissolved oxygen signal. The large observed spikes could be the result of nighttime mixing as previously observed by Holgerson et al. (2016) in small forest lakes or horizontal mixing, which is caused by differential heating/cooling of pelagic and littoral zones as described by Brothers et al. (2017). In Lake D, metabolism was estimated using oxygen data from one sensor only. In Lakes B and C, oxygen data from two sensors were used, performing the estimation procedure for each sensor and finally weighting the results by the volume represented by each sensor. We separated the water strata represented by each sensor at half the vertical distance between the sensors. We discarded days for which the correlation (Spearman’s rank) between the observed and predicted oxygen concentration was low ($r_s < 0.5$). Metabolism estimates are reported relative to lake surface areas as mmol O_2 m^{-2} day^{-1}. Respiration values are shown as negative in figures in order to aid visual interpretation.

Carbon dioxide and oxygen fluxes in Danish lakes

In each forest lake, the daily O_2 and CO_2 flux were calculated from the measured concentrations (O_2) or estimated partial pressure (CO_2) and the site specific relationships between k_{600} and wind. In order to enable a broader comparison of gas fluxes in lakes of variable surface areas, we used lake environmental monitoring data from a broad range of Danish lakes (NOVANA; Lauridsen et al. (2005)). In order to calculate CO_2 and O_2 fluxes, we used measurements of surface water temperature, alkalinity and pH to calculate CO_2 partial pressure following Weyhenmeyer et al. (2012) along with concurrent measurements of O_2 concentration and temperature (total of 4282 observations from 280 sites). To minimize the potential bias associated with estimation of CO_2 partial pressure from alkalinity and pH, we excluded observations from soft water lakes (alkalinity < 1 meq L^{-1}) and estimated CO_2 partial pressures exceeding 20.000 µatm (Abril et al. 2015). For calculation of the CO_2 flux, we used an atmospheric partial pressure of 400 µatm. With a grid size (20x20 km) of daily wind speeds from 1989 to 2010 (Scharling 2010) and information on lake size, the lake size and wind speed dependent k_{600} relationship from Vachon and Prairie (2013) combined with eq. 2 were used to calculate O_2 and CO_2 fluxes across the air-water interface.

Statistical methods

Because of forest sheltering, the wind speed measured at the meteorological station was adjusted to the individual lakes by fitting a linear model with measurements of wind speed, which were collected just above the water surface, as the response variable (n for each lake: A = 178, B = 10305, C= 3337, D = 15). Different linear models with and without an intercept and quadratic term were compared using F-tests; the variance explained is reported by the adjusted R^2 and the accuracy as the root mean squared error (RMSE).

To examine drivers of CO_2 flux and differences between seasons, we used measurements from the manual and automatic floating chambers along with relevant environmental variables (i.e. season, wind speed, water temperature and whether the water temperature was cooling or heating). We fitted mixed-effect models with “site” as a random effect using the “lme4” package and performed model selection using the Akaike Information Criterion (AIC; Burnham and Anderson (2002); Barton (2018)). The variance explained is reported as the marginal and conditional R^2, which is the variance explained by fixed factors only as well as both fixed and random factors, respectively (Nakagawa and Schielzeth 2013). The response variable (CO_2 flux) was log-transformed prior to analysis in order to ensure normality. Pairwise differences were examined using the “emmeans” package (Lenth 2018).

We compared the CO_2 estimated from alkalinity, pH and water temperature ($CO_{2(pH+alk)}$) to the headspace equilibrium concentration measured with floating chambers ($CO_{2(chamber)}$). Daily mean $CO_{2\ pH+alk}$ and $CO_{2(chamber)}$ concentrations were compared using standardized major axis regression (model II regression; Legendre (1998)) as both variables are measured with error.

We examined drivers of k_{600} using linear models in order to establish empirical relationships for estimation of ecosystem metabolism and calculation of long-term CO_2 flux. Data from Lakes B and C, which contained many measurements over the investigation period were employed. Only k_{600} measurements from the automatic floating chambers were used, as these were sampled throughout the daytime period, concurrently in the two lakes thus enabling site comparisons. The influence of key variables likely to influence k_{600} was tested including site, season, wind speed and whether the water column was heating or cooling. Because estimates of k_{600} during summer were missing, the spring level was used for model predictions instead. Moreover, for Lakes A and D, which were not included in the k_{600} modeling, the predicted values from Lake B were used instead.

All statistical analysis was performed in the statistical programming language R (R Core Team 2018).

Results

Site characteristics

Water chemistry in the investigated lakes was characterized by high levels of colored dissolved organic matter, medium to high chlorophyll *a* concentrations, high nutrient levels and high vertical light attenuation (Table 1). However, due to the shallow water, growth of submerged macrophytes took place from spring to fall. In Lake C, the biomass of *Potamogeton obtusifolius* was relatively high during fall with the canopy approaching the water surface before senescence during the winter.

Surrounding trees offered substantial sheltering compared to the meteorological station located in an open landscape. The dampening of wind speed just above the water surface relative to the meteorological station could be predicted from a model, which included a linear and squared term for each lake and the y-intercept set to zero ($R^2 = 0.87$, RMSE = 0.42 m s^{-1}). By including the squared term, the model fit was improved (F-test, F = 540, $p < 0.001$). On average, wind speed measured at the sites was reduced to 3% and 6% in the smallest Lakes A and D, respectively, and 28% and 35% in the larger Lakes B and C, respectively, compared to that in the open area (Fig. S1).

The lakes regularly showed diel temperature stratification with the water column being stratified during daytime and mixed at nighttime (Fig. 2). This phenomenon developed on most days from ice-off in April to late October. Outside this period, the lakes were either permanently vertically mixed or ice covered with inverse vertical stratification.

CO_2 partial pressure and CO_2 flux

High-frequency measurements of pH, water temperature and interpolated alkalinity time-series were used to construct a time-series of the waterside CO_2 partial pressure in three of the lakes (Fig. 3). Averaged across all the sampling points, the CO_2 partial pressure estimated from pH and alkalinity approached a 1:1 relationship, compared to measurements from floating chambers left to equilibrate on the water surface (Fig. S2). While the two methods act on different time scales due to a delayed response of the floating chamber to in-lake CO_2 partial pressure, the comparison supports the notion that the partial pressure estimated from alkalinity and pH is of the correct magnitude. Mostly, the surface water was supersaturated in CO_2 relative to the atmosphere with an overall median pressure of 4627 µatm. During summer, early fall and spring, the CO_2 partial pressure showed pronounced diel variability likely driven by photosynthesis of submerged macrophytes and phytoplankton (Fig. 3). Sudden spikes in surface water CO_2 were also observed in Lake D in fall, a period with increasing water level (Fig. 3, 7).

All direct measurements of CO_2 flux (n=1169) made with both manual and automatic floating chambers showed CO_2 emission to the atmosphere in agreement with the observed predominance of CO_2 supersaturation (Fig. 4). The best model of the CO_2 flux (AIC = 1494, AIC of second best model = 1502, $R^2_{marg} = 0.19$, $R^2_{cond} = 0.45$) included the fixed effects (parameter estimates and 95% confidence intervals on log scale) of water temperature (0.02 [0.008,0.034]), wind speed (linear term 0.59 [0.50,0.67], squared term -0.13 [-0.16,-0.10]), heating (in contrast to cooling; 0.14 [0.08,0.20]) and season. CO_2 evasion was significantly higher in summer than fall and spring ($p < 0.01$).

Gas exchange velocity

Gas exchange velocities calculated from measured CO_2 flux and CO_2 partial pressure gradients were generally low (median $k_{600} = 0.28$, range: 0.07-2.06 m day^{-1}), but increased at higher wind speeds (Fig. 5, C). The models of k_{600} improved by including a square term of wind speed (F-test, F = 8.13, $p < 0.001$). The relationship between k_{600} and wind speed differed between lakes (Fig. 5, A and B; significant interaction between wind speed and site, $p < 0.01$). There was also a significant effect of season (F-test, F = 186, $p < 0.001$) with k_{600} being higher in spring than winter ($p<0.001$) and fall ($p<0.001$). However, no significant effect of water column cooling or water column status (mixing, stably stratified and thermocline shallowing or deepening) on k_{600} was found. k_{600} values measured in this study were generally significantly different from those estimated by literature models (Fig. 5, C). In Lake B, all existing models differed from the measured k_{600} values (all p-values < 0.001). This was also the case in Lake C (all p-values < 0.01), except for the model of Read et al. (2012) (p-value = 0.97).

Ecosystem metabolism

Ecosystem metabolism was successfully estimated on 456 days in Lakes B, C and D. GPP and R were predominantly low and with distinct seasonal trends despite substantial day-to-day variations (Table 2). GPP and R were highest during spring, summer and early fall and decreased towards low winter values (Fig. S3). The higher rates of GPP and R during spring and summer were likely caused by higher light intensity and higher biomass of submerged macrophytes and phytoplankton. During ice cover, a diel oxygen signal was still present in Lakes B and C and low rates of GPP and R could be estimated. Mean oxygen saturation during ice cover was 60% and 53% in Lakes B and C, respectively. The relationship (slope) between GPP and R was systematically above 1.0 and R generally exceeded GPP (Table 2). Likewise, the interpolated background respiration (intercept) at zero GPP was positive. This finding suggests that R is supported by input of external organic matter. Consequently, NEP (= GPP - R) was generally negative throughout the year (Table 2, Fig. S3). This is in agreement with the systematic O_2 under saturation (Table 2). The strong ecosystem heterotrophy fuels the buildup of CO_2 and its subsequent release to the atmosphere.

Contribution of internal metabolism to CO_2 flux

Relating the CO_2 flux to NEP on a daily scale enables us to consider the contribution of aerobic in-lake metabolism to net CO_2 efflux. In the two-dimensional setting of daily net CO_2 flux and daily NEP, the observations are predominantly located in the space in which net CO_2 efflux exceeds the in-lake metabolic contribution to CO_2 formation (Fig. 6). The highest fluxes occurred in the larger Lakes B and C. For all months, the CO_2 efflux exceeded NEP reflecting CO_2 external input and, possibly, internal CO_2 generation by anaerobic sediment processes. During fall and winter, the CO_2 efflux generally increased, while NEP decreased. This suggests external hydrological CO_2 input. Moreover, differences between months followed changes in water level, particularly in Lake D, suggesting that the CO_2 efflux was maintained by an external, hydrologically mediated contribution to CO_2 in addition to the internal net CO_2 generation by aerobic ecosystem metabolism (Fig. 7).

Influence of lake size on the relationship between CO_2 and O_2 flux

Point estimations of CO_2 and O_2 flux from hundreds of Danish lakes were used to examine their interrelationship across lake size classes (Fig. 8). The density distribution showed that the CO_2 efflux relative to surface area increased with decreasing lake size. Small lakes acted as CO_2 sources while larger lakes were mainly CO_2 sinks. For O_2, the peaks of the density distributions of different lake sizes are not separated as well. However, O_2 invasion was predominant across all size classes, though O_2 evasion may occur periodically in both small and large lakes. From the imposed confidence ellipses, it is apparent that the relationship between CO_2 and O_2 fluxes differed between lake size classes. The confidence ellipses gradually moved closer towards the space with CO_2 evasion and O_2 invasion as lake size decreased. This space is shared by Lakes B, C and D, in which CO_2 evasion and O_2 invasion were highly pronounced.

Discussion

CO_2 partial pressure and efflux

We observed CO_2 supersaturation of surface waters in all four studied forest lakes with a median approximately ten times the atmospheric levels. High CO_2 levels have been found in other studies of small lakes. Sand-Jensen and Staehr (2007) observed 20-30 times CO_2 supersaturation as well as higher CO_2 levels in small forest lakes than in small lakes in open areas. Holgerson (2015) observed an average 20-fold CO_2 supersaturation in six ephemeral forest lakes. For a large number of small lakes and streams located in agricultural moraine soils in North Zealand (Denmark), ranges of median CO_2 supersaturation levels were 5-15 and 9-18-fold, respectively (Sand-Jensen and Staehr 2009; Sand-Jensen and Staehr 2012). Soil microbial activity is lower in boreal areas, but nevertheless, three times supersaturation of median CO_2 partial pressure was observed in boreal lakes and streams (Weyhenmeyer et al. 2012). The high CO_2 supersaturation in small lakes and streams is often accompanied by high CH_4 production (Wallin et al. 2017; Grinham et al. 2018), which corroborates the importance of these highly abundant habitats in global carbon budgets (Holgerson and Raymond 2016).

While the low pH of Lake A prevented calculation of an unbiased CO_2 partial pressure from alkalinity, the CO_2 levels are likely similar or higher than the partial pressure observed in the other three forest lakes. We only calculated CO_2 levels close to (Lake C) or slightly below (Lake B) atmospheric saturation during periods of high macrophyte biomass and photosynthesis. Moreover, all floating chamber measurements showed CO_2 effluxes from surface waters in accordance with the predominant CO_2 supersaturation. The high number of direct flux measurements using floating chambers (n = 1169) and the extensive coverage of seasonal to daily variations, support the conclusion that CO_2 supersaturation and CO_2 efflux are the predominant state throughout the year as expected for the forest lakes (hypothesis 1). The calculations of CO_2 partial pressures may be biased at low alkalinity and low pH, which is why we avoided CO_2 calculations in Lake A, whereas alkalinity and pH were intermediate in Lakes B, C and D. Indeed, calculations of CO_2 partial pressure in surface waters from measured alkalinity and pH in these lakes yielded a 1:1

relationship to partial pressure measured in floating chambers in the range of 2000-8000 µatm with some scatter (Fig. S2). The variability around the 1:1 line is likely influenced by the long response time of the floating chambers to attain full air-water equilibrium due to the observed low gas exchange velocities (Bastviken et al. 2015). Overall, these findings support the validity of estimating waterside CO_2 partial pressure from pH and alkalinity and the calculations of gas exchange velocity from measured gas fluxes in our study lakes. The CO_2 flux measured directly using floating chambers and that calculated using the modelled gas exchange velocity and estimated CO_2 partial pressure are strongly correlated (Pearson-r = 0.55, $p < 0.001$, RMSE = 1.0 mmol m^{-2} day^{-1}). Moreover, other studies have found good correspondence between calculated (from pH and alkalinity) and direct measurements of CO_2 concentrations in surface waters of intermediate to high alkalinity and pH, which resembles the chemical conditions in our forest lakes B, C and D (Frankignoulle and Borges 2001; Abril et al. 2015).

The main growth season from late spring to fall had higher diel variability of CO_2 concentrations and lake chemistry compared to the winter season. The growing macrophyte biomass may contribute to this higher diel variability through its metabolism (Fig. S3, Martinsen et al. (2017)) and its physical dissipation of turbulence, which promotes daytime stratification followed by nighttime surface cooling and convective mixing (Andersen et al. 2017). When photosynthesis is restricted to surface waters due to vertical stratification, concentrations of dissolved inorganic carbon (DIC), CO_2 and O_2 will undergo more extensive diel changes. In small lakes of low wind exposure, steep vertical light attenuation caused by macrophytes, colored dissolved organic matter and phytoplankton commonly induce recurring daytime stratification and nocturnal convective mixing (Dale and Gillespie 1977; Martinsen et al. 2019). Diel changes of DIC and CO_2 are particularly profound when dense macrophyte stands combine photosynthetic use of CO_2 and bicarbonate (HCO_3^-) with formation of calcium carbonate on plant surfaces and sedimentation of calcite crystals from surface to bottom waters, during daytime (Andersen et al. 2019). Calcite crystals can re-dissolve in CO_2-rich bottom waters and inorganic carbon be recirculated during nocturnal mixing. Calcification in surface waters and dissolution of carbonate in bottom waters are probably insignificant in the investigated forest lakes, because of the low surface pH (< 8; Table 1) and the photosynthetic rates being too low to induce calcium carbonate precipitation.

Gas exchange velocity in small lakes

We calculated the gas exchange velocity (k_{600}) from measurements of gas flux and surface water CO_2 partial pressure.

Our gas exchange velocities were low compared to those in medium and large lakes, but resembled values for other small lakes <0.01 km^2 (Holgerson et al. 2017). The low gas exchange velocity for small lakes is expected due to sheltering by landscape contours, surrounding trees or emergent vegetation as well as a short fetch across the lake surface. The relationship between gas exchange velocity and wind speed differed between Lakes B and C – potentially due to differences in lake sizes and shapes (Vachon and Prairie 2013) or associated attributes, such as atmospheric and near-surface stability (MacIntyre et al. 2018). We also found differences in gas exchange velocity between seasons with higher values during spring. One major seasonal difference was the lower macrophyte density in spring compared to summer and fall. Submerged macrophytes are known to effectively dissipate wind induced turbulence (Herb and Stefan 2005). The inclusion of measurements of macrophyte height, biomass and type could improve future studies on turbulence and gas exchange velocity in small lakes. Moreover, variable concentrations of phytoplankton and colored dissolved organic matter may influence vertical light attenuation and water column stability and, thereby, the influence of wind speed on gas exchange velocity, particularly at the low wind speeds experienced in small, sheltered lakes (Laurion et al. 2010).

As a consequence of the reduced influence of wind-induced mixing in small forest lakes, we expected the relative contribution of convective mixing to increase (Read et al. 2012) and result in poor performance of existing gas exchange models using wind speed as the sole predictor (hypothesis 2). However, we did not find a significant effect of surface cooling on gas exchange velocity, while the effect of wind speed was stronger (Fig. 5). Despite this, the wind-based empirical models of Cole and Caraco (1998) and Crusius and Wanninkhof (2003) predicted either too high or too low gas exchange velocities, while the model of Read et al. (2012), which includes convective mixing, predicted rates within the same range as the measured values (Fig. 5). This is surprising as we did not observe a significant effect of surface cooling as a proxy of convection. Using whole-lake tracer additions in four small forest lakes, Holgerson et al. (2017) reported gas exchange velocities between 0.19 and 0.72 m day^{-1}, no effect of surface cooling and generally weak relationships to other environmental variables. In contrast, MacIntyre et al. (2018), by applying acoustic Doppler velocimetry in a small arctic lake, found an increase in near-surface turbulence during cooling, which should increase gas exchange velocity as well. This inconsistency between different studies and models to quantify gas exchange velocity and the importance of convection in small lakes is challenging, but may arise from differences in methodology or the influence of local field conditions. Regarding methodology, Podgrajsek et al. (2014) compared eddy-covariance and floating chambers, and reported that floating chambers appeared to miss convection in contrast to eddy-covariance, which showed a nighttime increase in CO_2 flux that they attributed to nocturnal surface cooling and convection. However, in other studies, floating chambers have shown good agreement with measurements by other methods (Gålfalk et al. 2013) and logically, floating chambers should be able to pick up the influence of both wind and convection on surface turbulence as well as subsequent gas exchange velocity. In order to unravel the inconsistencies, simultaneous measurements of gas exchange velocity, surface turbulence and the driving forces (i.e. wind or surface cooling) it is necessary to use a combination of methods. In our study lakes, the influence of convection was not important and gas exchange velocity appeared to be primarily driven by wind. The role of convection in otherwise similar appearing small lakes might differ due to factors such as sheltering or submerged vegetation which in turn influence surface heat fluxes (Herb and Stefan 2005; Poindexter and Variano 2013).

Lake metabolism and CO_2 flux

We quantified the CO_2 flux and net ecosystem metabolism (NEP) in order to examine the contribution of internal metabolism to the air-water CO_2 flux. We also calculated the O_2 flux to enable comparison with the CO_2 flux, though NEP is likely the most direct measure of daily aerobic metabolic balance between photosynthesis and respiration. The three small forest lakes exhibited strong heterotrophy, which is expected in small forest lakes and brown-water lakes in general (Sand-Jensen and Staehr 2007; Ask et al. 2012). The daily CO_2 efflux usually exceeded the net quantity of CO_2 produced within the system by aerobic metabolism according to measured NEP (Fig. 6). In Lakes B and C, annual CO_2 effluxes were 37.6 and 35 mol m^{-2} and surpassed annual net CO_2 formation by ecosystem metabolism (12 and 13.9 mol m^{-2} using a respiratory quotient of 1) by 3.1 and 2.5 times, respectively (Table 2). The deficit is likely covered by a combination of hydrological CO_2 input and internal anaerobic CO_2 formation of unknown magnitudes. Groundwater input or surface runoff deliver water supersaturated with CO_2, while anaerobic metabolism within the system generates CO_2 without consuming O_2 (Torgersen and Branco 2007). Wilkinson et al. (2016) also found an excess CO_2 efflux (two times higher) relative to what could be generated within the system, even when accounting for the potential contribution by anaerobic metabolism. If the excess CO_2 flux was to be maintained by only hydrological input in the lakes investigated in this study, it would require an unrealistically short residence time. Covering the deficit solely by methane fermentation by equal molar rates of methane and CO_2 formation require annual rates exceeding 21 mol CH_4 m^{-2}. Lake methane fluxes in this range are in the very high end of previous published values (DelSontro et al. 2016; Grinham et al. 2018), which suggests a shared contribution of hydrological and anaerobic processes.

Other anaerobic processes than methane fermentation may contribute to the excess CO_2 flux. External input of nitrate, sulfate and oxidized iron and manganese, followed by anaerobic respiration of organic matter, will produce surplus CO_2 relative to O_2. However, dissolved inorganic nitrogen input from the primarily water-saturated and anoxic forest soils will mainly be as ammonium and not as nitrate. High ammonium and low nitrate concentrations in the forest lakes support this assumption (Table 2). Nitrification of ammonium by oxygen followed by anaerobic denitrification of nitrate within the lake does not produce a CO_2 surplus relative to O_2 consumption, but a deficit. Likewise, a small sulfate input from water-saturated forest soils will only release CO_2 without O_2 consumption, if sulfide formed by anaerobic degradation of organic matter becomes permanently buried in reduced form (e.g. iron sulfides) in the sediments and is not re-oxidized to sulfate in the water. Groundwater input of oxidized iron and manganese is unlikely because both forms are insoluble. Water received as intermittent surface flow across the forest floor may contain oxidation capacity, but was not accounted for. Thus, the relative magnitude of hydrological CO_2 input and anaerobic CO_2 formation requires further investigation.

Scaling of ecosystem size and function

Point estimations of CO_2 and O_2 fluxes from hundreds of Danish lakes showed that small lakes systematically acted as CO_2 sources to the atmosphere, while larger lakes were mainly CO_2 sinks. The data were collected as part of the national environmental program and samples were only collected during daytime. However, using a subset of the data from late morning (8AM-12PM), where the concentrations approximates the diel mean (Sand-Jensen and Staehr 2007), did not alter the resulting confidence ellipses or density distributions. The pronounced heterotrophy of small lakes, as exemplified by the studied forest lakes, is driven by a large contact zone with the terrestrial surroundings and high input of degradable organic material relative to lake surface area (hypothesis 3, Downing (2010)). In addition, lake primary production is constrained by shading from terrestrial vegetation and colored dissolved organic matter (CDOM) in the water. Higher CO_2 supersaturation, CO_2 efflux and CDOM concentrations and lower phytoplankton biomass and GPP are also evident in the comparison of small forest lakes with small open land lakes (Sand-Jensen and Staehr 2007). In contrast to the forest lakes investigated here which had higher CO_2 efflux during summer, larger Danish lakes were mainly CO_2 sinks, especially during summer. This is likely because they are mainly eutrophic, shallow and support high phytoplankton production (Trolle et al. 2012). High phytoplankton production generates CO_2 undersaturation and high pH, which facilitates chemically enhanced CO_2 uptake (Bade and Cole 2006). The number of samples was higher during spring and summer, which may increase CO_2 uptake relative to CO_2 release in the annual balance, because CO_2 uptake is promoted by plant growth during spring and summer, while CO_2 release is promoted by proportionally greater organic degradation than photosynthesis during fall and winter.

For O_2 fluxes, the peaks in the density distributions of different lake sizes are not as well separated as CO_2 fluxes and NEP. However, O_2 invasion dominated across all size classes, though O_2 evasion occurred periodically in both small and large lakes during periods of intensive photosynthesis in spring and summer. This finding reflects that during periods of net autotrophy (GPP > R) and O_2 efflux, CO_2 efflux may continue as a result of external CO_2 input, anaerobic sediment respiration and CO_2 formation by calcium carbonate deposition (McConnaughey et al. (1994); $Ca^{2+} + 2\ HCO_3^- \rightarrow CaCO_3 + CO_2 + H_2O$). The imposed confidence ellipses for the Danish lakes gradually moved closer towards the space with CO_2 evasion and O_2 invasion as lake area decreased. This space was shared by the studied forest lakes in which CO_2 evasion and O_2 invasion were very pronounced.

Conclusions

Four small forest lakes were markedly CO_2 supersaturated and emitted CO_2 to the atmosphere in all measurements. High CO_2 emission was supported only in part by in-lake aerobic net ecosystem production, which suggests additional CO_2 sources (e.g., hydrological CO_2 input and anaerobic respiration). This substantial deficit has been observed by others and requires future focus. A national scale analysis showed that with decreasing lake surface area, CO_2 flux increased and the relationship between CO_2 and O_2 flux moved towards excess CO_2 efflux. Despite the gas exchange velocity generally increasing with lake surface area, higher CO_2 fluxes are sustained by marked CO_2 supersaturation in small lakes. The national scale pattern revealed a shift from large eutrophic lakes with net O_2 release and net CO_2 uptake to small lakes, forest lakes in particular, with net O_2 uptake and net CO_2 release, likely a consequence of increasing input of dissolved CO_2 and organic matter from the tightly connected terrestrial environment to small lakes.

References:

Abril G et al. (2015) Large overestimation of pCO2 calculated from pH and alkalinity in acidic, organic-rich freshwaters Biogeosciences 12:67-78 doi:10.5194/bg-12-67-2015

Andersen MR, Kragh T, Martinsen KT, Kristensen E, Sand-Jensen K (2019) The carbon pump supports high primary production in a shallow lake Aquat Sci 81:24 doi:10.1007/s00027-019-0622-7

Andersen MR, Sand-Jensen K, Iestyn Woolway R, Jones ID (2017) Profound daily vertical stratification and mixing in a small, shallow, wind-exposed lake with submerged macrophytes Aquat Sci 79:395-406 doi:10.1007/s00027-016-0505-0

Ask J, Karlsson J, Jansson M (2012) Net ecosystem production in clear-water and brown-water lakes Global Biogeochemical Cycles 26:n/a-n/a doi:10.1029/2010GB003951

Bade DL, Cole JJ (2006) Impact of chemically enhanced diffusion on dissolved inorganic carbon stable isotopes in a fertilized lake Journal of Geophysical Research: Oceans 111 doi:10.1029/2004jc002684

Barton K (2018) MuMIn: Multi-Model Inference, R package version 1.40.4. https://CRAN.R-project.org/package=MuMIn.

Bastviken D, Cole J, Pace M, Tranvik L (2004) Methane emissions from lakes: Dependence of lake characteristics, two regional assessments, and a global estimate Global Biogeochemical Cycles 18 doi:10.1029/2004gb002238

Bastviken D, Sundgren I, Natchimuthu S, Reyier H, Gålfalk M (2015) Technical Note: Cost-efficient approaches to measure carbon dioxide (CO 2) fluxes and concentrations in terrestrial and aquatic environments using mini loggers Biogeosciences 12:3849-3859 doi:10.5194/bg-12-3849-2015

Brothers S, Kazanjian G, Köhler J, Scharfenberger U, Hilt S (2017) Convective mixing and high littoral production established systematic errors in the diel oxygen curves of a shallow, eutrophic lake Limnol Oceanogr Methods 15:429-435 doi:10.1002/lom3.10169

Burnham KP, Anderson DR (2002) Model Selection and Multimodel Inference: A Practical Information-Theoretic Approach. Springer, New York

Cole JJ, Bade DL, Bastviken D, Pace ML, Van de Bogert M (2010) Multiple approaches to estimating air-water gas exchange in small lakes Limnol Oceanogr Methods 8:285-293 doi:10.4319/lom.2010.8.285

Cole JJ, Caraco NF (1998) Atmospheric exchange of carbon dioxide in a low-wind oligotrophic lake measured by the addition of SF6 Limnol Oceanogr 43:647-656 doi:10.4319/lo.1998.43.4.0647

Cole JJ, Caraco NF, Kling GW, Kratz TK (1994) Carbon dioxide supersaturation in the surface waters of lakes Science 265:1568-1570 doi:10.1126/science.265.5178.1568

Crusius J, Wanninkhof R (2003) Gas transfer velocities measured at low wind speed over a lake Limnol Oceanogr 48:1010-1017 doi:10.4319/lo.2003.48.3.1010

Dale HM, Gillespie TJ (1977) Influence of submersed aquatic plants on temperature-gradients in shallow-water bodies Canadian Journal of Botany 55:2216-2225 doi:10.1139/b77-251

DelSontro T, Boutet L, St-Pierre A, del Giorgio PA, Prairie YT (2016) Methane ebullition and diffusion from northern ponds and lakes regulated by the interaction between temperature and system productivity Limnol Oceanogr 61 doi:10.1002/lno.10335

DMI (2017) Danish Meterological Institute. http://www.dmi.dk/vejr/arkiver/vejrarkiv/. Accessed December 2017

Downing J et al. (2006) The global abundance and size distribution of lakes, ponds, and impoundments Limnol Oceanogr 51:2388-2397 doi:10.4319/lo.2006.51.5.2388

Downing JA (2010) Emerging global role of small lakes and ponds: little things mean a lot Limnetica 29:9-24

Dugan H et al. (2016) Consequences of gas flux model choice on the interpretation of metabolic balance across 15 lakes Inland Waters 6:581-592 doi:10.1080/iw-6.4.836

Finlay K, Leavitt P, Patoine A, Patoine A, Wissel B (2010) Magnitudes and controls of organic and inorganic carbon flux through a chain of hard-water lakes on the northern Great Plains Limnol Oceanogr 55:1551-1564 doi:10.4319/lo.2010.55.4.1551

Frankignoulle M, Borges AV (2001) Direct and indirect pCO 2 measurements in a wide range of pCO 2 and salinity values (the Scheldt estuary) Aquatic Geochemistry 7:267-273 doi:10.1023/a:1015251010481

Gran G (1952) Determination of the equivalence point in potentiometric titrations. Part II Analyst 77:661-671 doi:10.1039/an9527700661

Grinham A et al. (2018) The importance of small artificial water bodies as sources of methane emissions in Queensland, Australia Hydrology and Earth System Sciences 22:5281-5298 doi:10.5194/hess-2018-294

Guérin F et al. (2007) Gas transfer velocities of CO2 and CH4 in a tropical reservoir and its river downstream J Mar Syst 66:161-172 doi:10.1016/j.jmarsys.2006.03.019

Gålfalk M, Bastviken D, Fredriksson S, Arneborg L (2013) Determination of the piston velocity for water-air interfaces using flux chambers, acoustic Doppler velocimetry, and IR imaging of the water surface Journal of Geophysical Research: Biogeosciences 118:770-782 doi:10.1002/jgrg.20064

Hanson PC, Bade DL, Carpenter SR, Kratz TK (2003) Lake metabolism: Relationships with dissolved organic carbon and phosphorus Limnol Oceanogr 48:1112-1119 doi:10.4319/lo.2003.48.3.1112

Heiskanen JJ, Mammarella I, Haapanala S, Pumpanen J, Vesala T, MacIntyre S, Ojala A (2014) Effects of cooling and internal wave motions on gas transfer coefficients in a boreal lake 2014 doi:10.3402/tellusb.v66.22827

Herb WR, Stefan HG (2005) Dynamics of vertical mixing in a shallow lake with submersed macrophytes Water Resources Research 41 doi:10.1029/2003wr002613

Holgerson MA (2015) Drivers of carbon dioxide and methane supersaturation in small, temporary ponds Biogeochemistry 124:305-318 doi:10.1007/s10533-015-0099-y

Holgerson MA, Farr ER, Raymond PA (2017) Gas transfer velocities in small forested ponds Journal of Geophysical Research: Biogeosciences 122:1011-1021 doi:10.1002/2016JG003734

Holgerson MA, Raymond PA (2016) Large contribution to inland water CO2 and CH4 emissions from very small ponds Nature Geoscience 9:222-226 doi:10.1038/ngeo2654

Holgerson MA, Zappa CJ, Raymond PA (2016) Substantial overnight reaeration by convective cooling discovered in pond ecosystems Geophys Res Lett 43:8044-8051 doi:10.1002/2016gl070206

Hotchkiss E et al. (2015) Sources of and processes controlling CO 2 emissions change with the size of streams and rivers Nature Geoscience 8:696 doi:10.1038/ngeo2507

Imberger J (1985) The diurnal mixed layer Limnol Oceanogr 30:737-770 doi:10.4319/lo.1985.30.4.0737

Jespersen A-M, Christoffersen K (1987) Measurements of chlorophyll—a from phytoplankton using ethanol as extraction solvent Archiv für Hydrobiologie 109:445-454

Jähne B, Münnich KO, Bösinger R, Dutzi A, Huber W, Libner P (1987) On the parameters influencing air-water gas exchange Journal of Geophysical Research 92:1937-1949 doi:10.1029/jc092ic02p01937

Jørgensen SE, Bendoricchio G (2001) Fundamentals of ecological modelling vol 21. Developments in environmental modelling. Elsevier, Amsterdam

Kling GW, Kipphut GW, Miller MC (1991) Arctic lakes and streams as gas conduits to the atmosphere: implications for tundra carbon budgets Science 251:298-301 doi:10.1126/science.251.4991.298

Kragh T, Andersen MR, Sand-Jensen K (2017) Profound afternoon depression of ecosystem production and nighttime decline of respiration in a macrophyte-rich, shallow lake Oecologia 185:157-170 doi:10.1007/s00442-017-3931-3

Lauridsen TL, Søndergaard M, Jensen JP, Jeppesen E (2005) Investigations in lakes (in danish). Danish Center for Environment,

Laurion I, Vincent WF, MacIntyre S, Retamal L, Dupont C, Francus P, Pienitz R (2010) Variability in greenhouse gas emissions from permafrost thaw ponds Limnol Oceanogr 55:115-133 doi:10.4319/lo.2010.55.1.0115

Legendre P (1998) Model II regression user's guide, R edition R Vignette

Lenth R (2018) emmeans: Estimated Marginal Means, aka Least-Squares Means, R package version 1.2.2. https://CRAN.R-project.org/package=emmeans.

Maberly SC, Barker PA, Stott AW, De Ville MM (2013) Catchment productivity controls CO 2 emissions from lakes Nature Climate Change 3:391 doi:10.1038/nclimate1748

MacIntyre S, Crowe AT, Cortés A, Arneborg L (2018) Turbulence in a small arctic pond Limnol Oceanogr 63:2337-2358 doi:10.1002/lno.10941

MacIntyre S, Wanninkhof R, Chanton J (1995) Trace gas exchange across the air-water interface in freshwater and coastal marine environments. In: Matson PA, Harris RC (eds) Biogenic trace gases: Measuring emissions from soil and water, vol 52-97. Blackwell,

Marcé R, Obrador B, Morguí J-A, Riera JL, López P, Armengol J (2015) Carbonate weathering as a driver of CO 2 supersaturation in lakes Nature Geoscience 8:107 doi:10.1038/ngeo2341

Marotta H, Duarte CM, Pinho L, Enrich-Prast A (2011) Rainfall leads to increased pCO2 in Brazilian coastal lakes

Martinsen KT, Andersen MR, Kragh T, Sand-Jensen K (2017) High rates and close diel coupling of primary production and ecosystem respiration in small, oligotrophic lakes Aquat Sci 79:995-1007 doi:10.1007/s00027-017-0550-3

Martinsen KT, Andersen MR, Sand-Jensen K (2019) Water temperature dynamics and the prevalence of daytime stratification in small temperate shallow lakes Hydrobiologia 826:247-262 doi:10.1007/s10750-018-3737-2

Martinsen KT, Kragh T, Sand-Jensen K (2018) Technical note: A simple and cost-efficient automated floating chamber for continuous measurements of carbon dioxide gas flux on lakes Biogeosciences 15:5565-5573 doi:10.5194/bg-15-5565-2018

McConnaughey TA, LaBaugh JW, Striegl RG, Reddy MM, Schuster PF, Carter V (1994) Carbon budget for a groundwater-fed lake: Calcification supports summer photosynthesis Limnol Oceanogr 39:1319-1332 doi:10.4319/lo.1994.39.6.1319

McDonald CP, Stets EG, Striegl RG, Butman D (2013) Inorganic carbon loading as a primary driver of dissolved carbon dioxide concentrations in the lakes and reservoirs of the contiguous United States Global Biogeochemical Cycles 27:285-295 doi:10.1002/gbc.20032

Nakagawa S, Schielzeth H (2013) A general and simple method for obtaining R2 from generalized linear mixed-effects models Methods in Ecology and Evolution 4:133-142 doi:10.1111/j.2041-210x.2012.00261.x

Natchimuthu S, Sundgren I, Gålfalk M, Klemedtsson L, Bastviken D (2017) Spatiotemporal variability of lake pCO2 and CO2 fluxes in a hemiboreal catchment Journal of Geophysical Research: Biogeosciences 122:30-49 doi:10.1002/2016JG003449

Podgrajsek E, Sahlée E, Bastviken D, Holst J, Lindroth A, Tranvik L, Rutgersson A (2014) Comparison of floating chamber and eddy covariance measurements of lake greenhouse gas fluxes Biogeosciences 11:4225 doi:10.5194/bg-11-4225-2014

Poindexter CM, Variano EA (2013) Gas exchange in wetlands with emergent vegetation: The effects of wind and thermal convection at the air-water interface Journal of Geophysical Research: Biogeosciences 118:1297-1306

R Core Team (2018) R: A language and environment for statistical computing. Vienna, R Foundation for Statistical Computing.

Read JS et al. (2012) Lake-size dependency of wind shear and convection as controls on gas exchange Geophys Res Lett 39 doi:10.1029/2012gl051886

Read JS et al. (2011) Derivation of lake mixing and stratification indices from high-resolution lake buoy data Environ Model Software 26:1325-1336 doi:10.1016/j.envsoft.2011.05.006

Sand-Jensen K, Staehr PA (2007) Scaling of pelagic metabolism to size, trophy and forest cover in small Danish lakes Ecosystems 10:128-142 doi:10.1007/s10021-006-9001-z

Sand-Jensen K, Staehr PA (2009) Net heterotrophy in small Danish lakes: a widespread feature over gradients in trophic status and land cover Ecosystems 12:336-348 doi:10.1007/s10021-008-9226-0

Sand-Jensen K, Staehr PA (2012) CO2 dynamics along Danish lowland streams: water–air gradients, piston velocities and evasion rates Biogeochemistry 111:615-628 doi:10.1007/s10533-011-9696-6

Scharling M (2010) Climate Grid Denmark. Danish Meteorological Institute,

Solomon CT et al. (2013) Ecosystem respiration: drivers of daily variability and background respiration in lakes around the globe Limnol Oceanogr 58:849-866 doi:10.4319/lo.2013.58.3.0849

Staehr PA, Baastrup-Spohr L, Sand-Jensen K, Stedmon C (2012) Lake metabolism scales with lake morphometry and catchment conditions Aquat Sci 74:155-169 doi:10.1007/s00027-011-0207-6

Striegl RG, Michmerhuizen CM (1998) Hydrologic influence on methane and carbon dioxide dynamics at two north-central Minnesota lakes Limnol Oceanogr 43:1519-1529 doi:10.4319/lo.1998.43.7.1519

Sørensen J, Jørgensen BB, Revsbech NP (1979) A comparison of oxygen, nitrate, and sulfate respiration in coastal marine sediments Microb Ecol 5:105-115

Torgersen T, Branco B (2007) Carbon and oxygen dynamics of shallow aquatic systems: Process vectors and bacterial productivity Journal of Geophysical Research: Biogeosciences 112 doi:10.1029/2007jg000401

Torgersen T, Branco B (2008) Carbon and oxygen fluxes from a small pond to the atmosphere: Temporal variability and the CO2/O2 imbalance Water Resources Research 44 doi:10.1029/2006WR005634

Trolle D, Staehr PA, Davidson TA, Bjerring R, Lauridsen TL, Søndergaard M, Jeppesen E (2012) Seasonal dynamics of CO2 flux across the surface of shallow temperate lakes Ecosystems 15:336-347 doi:10.1007/s10021-011-9513-z

University of Copenhagen (1992) Limnological methods (in danish). Freshwater Biological Laboratory. Akademisk Forlag, Copenhagen

Vachon D, Prairie YT (2013) The ecosystem size and shape dependence of gas transfer velocity versus wind speed relationships in lakes Can J Fish Aquat Sci 70:1757-1764 doi:10.1139/cjfas-2013-0241

Vachon D, Prairie YT, Cole JJ (2010) The relationship between near-surface turbulence and gas transfer velocity in freshwater systems and its implications for floating chamber measurements of gas exchange Limnol Oceanogr 55:1723 doi:10.4319/lo.2010.55.4.1723

Wallin MB et al. (2017) Carbon dioxide and methane emissions of Swedish low-order streams—a national estimate and lessons learnt from more than a decade of observations Limnology and Oceanography Letters doi:10.1002/lol2.10061

Wanninkhof R (1992) Relationship between wind speed and gas exchange over the ocean J Geophys Res-Oceans 97:7373-7382 doi:10.1029/92jc00188

Weyhenmeyer GA, Kortelainen P, Sobek S, Müller R, Rantakari M (2012) Carbon dioxide in boreal surface waters: a comparison of lakes and streams Ecosystems 15:1295-1307 doi:10.1007/s10021-012-9585-4

Weyhenmeyer GA, Kosten S, Wallin MB, Tranvik LJ, Jeppesen E, Roland F (2015) Significant fraction of CO 2 emissions from boreal lakes derived from hydrologic inorganic carbon inputs Nature Geoscience 8:933 doi:10.1038/ngeo2582

Wilkinson GM, Buelo CD, Cole JJ, Pace ML (2016) Exogenously produced CO2 doubles the CO2 efflux from three north temperate lakes Geophys Res Lett 43:1996-2003 doi:10.1002/2016gl067732

Wilkinson GM, Pace ML, Cole JJ (2013) Terrestrial dominance of organic matter in north temperate lakes Global Biogeochemical Cycles 27:43-51 doi:10.1029/2012gb004453

Winslow LA et al. (2016) LakeMetabolizer: An R package for estimating lake metabolism from free-water oxygen using diverse statistical models Inland Waters 6:622-636

Woolway RI et al. (2016) Diel Surface Temperature Range Scales with Lake Size PLoS ONE 11:e0152466 doi:10.1371/journal.pone.0152466

This is a post-peer-review, pre-copyedit version of an article published in Aquatic Sciences. The final authenticated version is available online at: https://doi.org/10.1007/s00027-019-0682-8

Figure legends

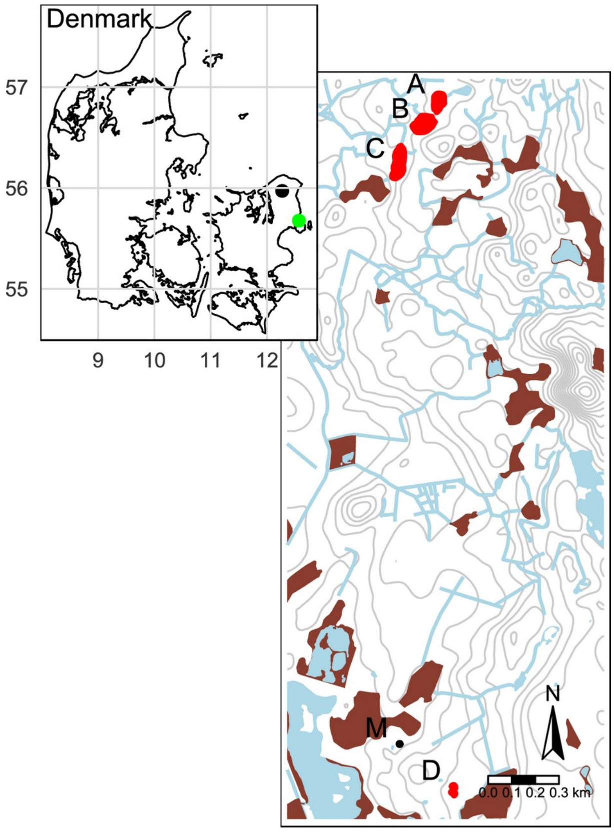

Fig. 1 Map of study site and location (black) of the four small lakes in Grib Forest in North Zealand (Denmark with Copenhagen shown in green). The study sites are shown in red and "M" is the meteorological station. Also shown are streams and lakes in blue, wetlands in brown and elevation contour lines (2.5 m) in grey

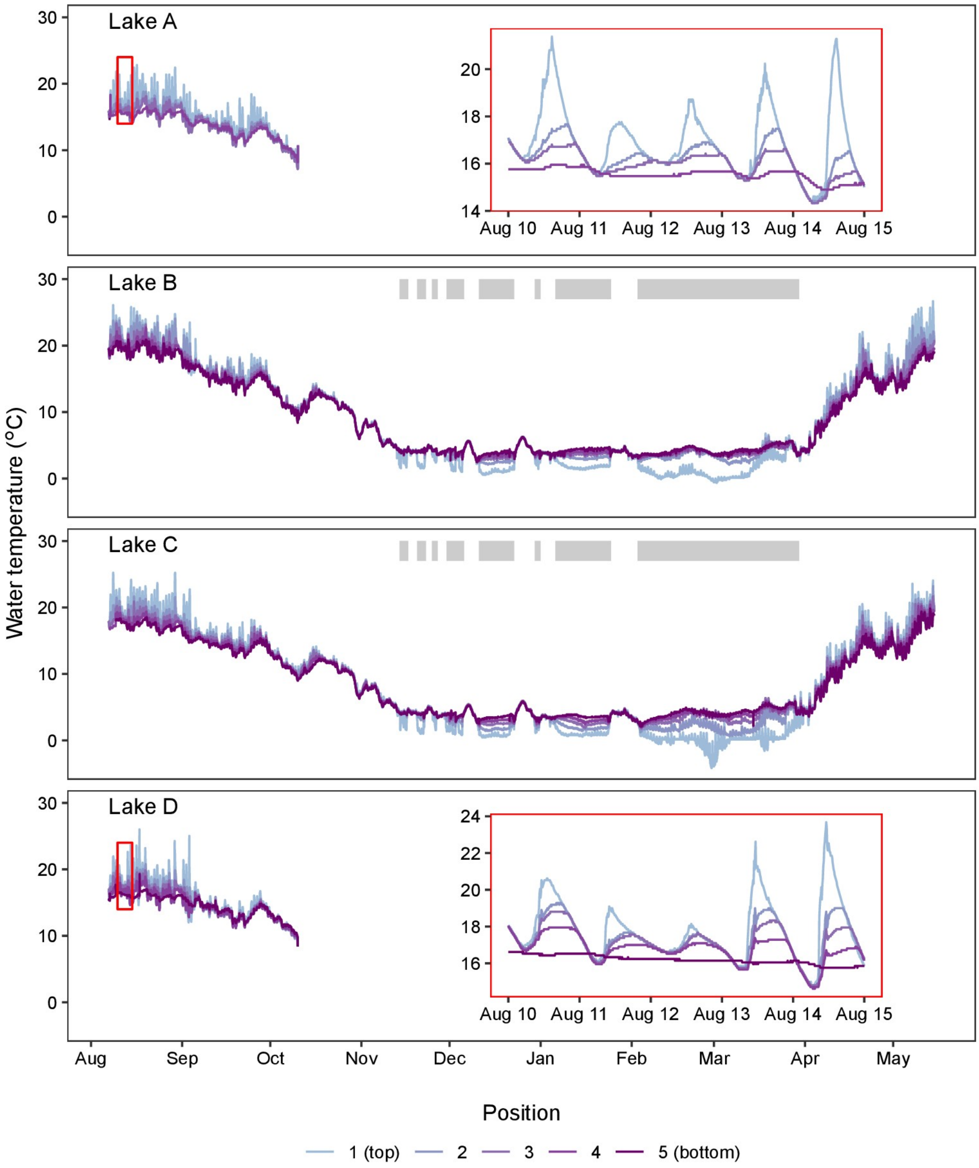

Fig. 2 High-frequency measurements of water temperature in four small forest lakes over the year. Lines are colored according to their vertical position in the water column. In Lakes A and D, two five-day periods are provided as zoom insets (red rectangles). Grey boxes show periods of ice cover

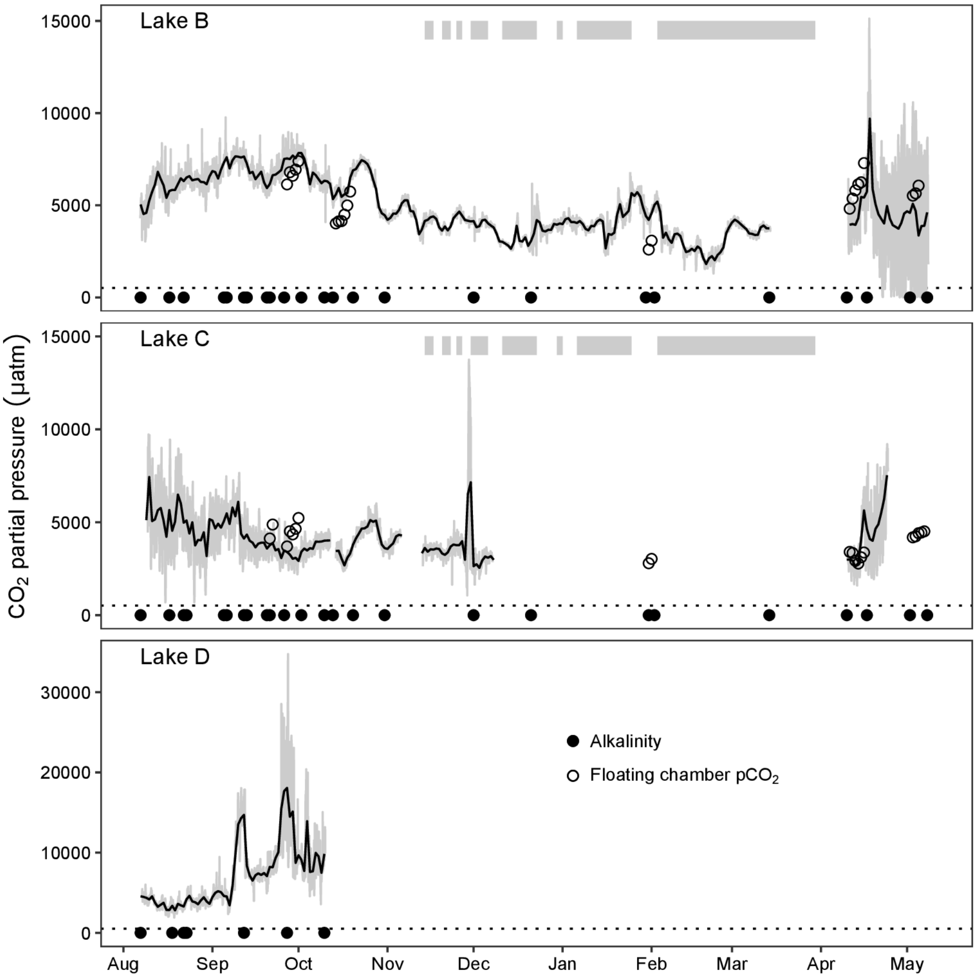

Fig. 3 High-frequency measurements of CO_2 partial pressure (grey line) and daily mean (black line) in four small forest lakes over the year. Days of water sampling for alkalinity measurements are marked (closed points) and measurements of CO_2 partial pressure (open points) along with the mean atmospheric CO_2 partial pressure (dotted line). Gray boxes show winter periods of ice cover

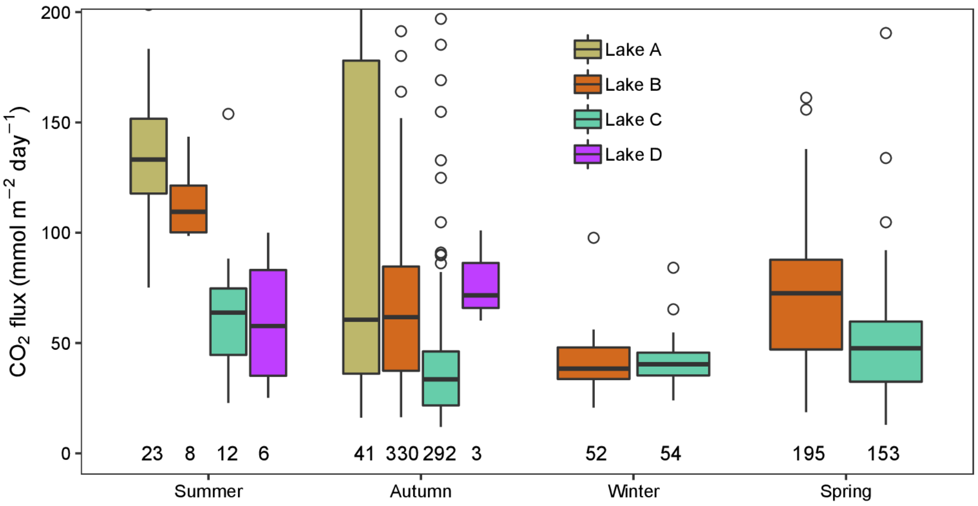

Fig. 4 Floating chamber measurements of seasonal CO$_2$ emission from water to air in four small forest lakes. Box plots show median (solid horizontal line), 25% and 75% quartile (upper and lower hinge), vertical lines extend 1.5 times the inter-quartile range and observations outside this range are points. Number of observations is denoted below each box. 23 data points are outside (higher) than the shown y-axis range

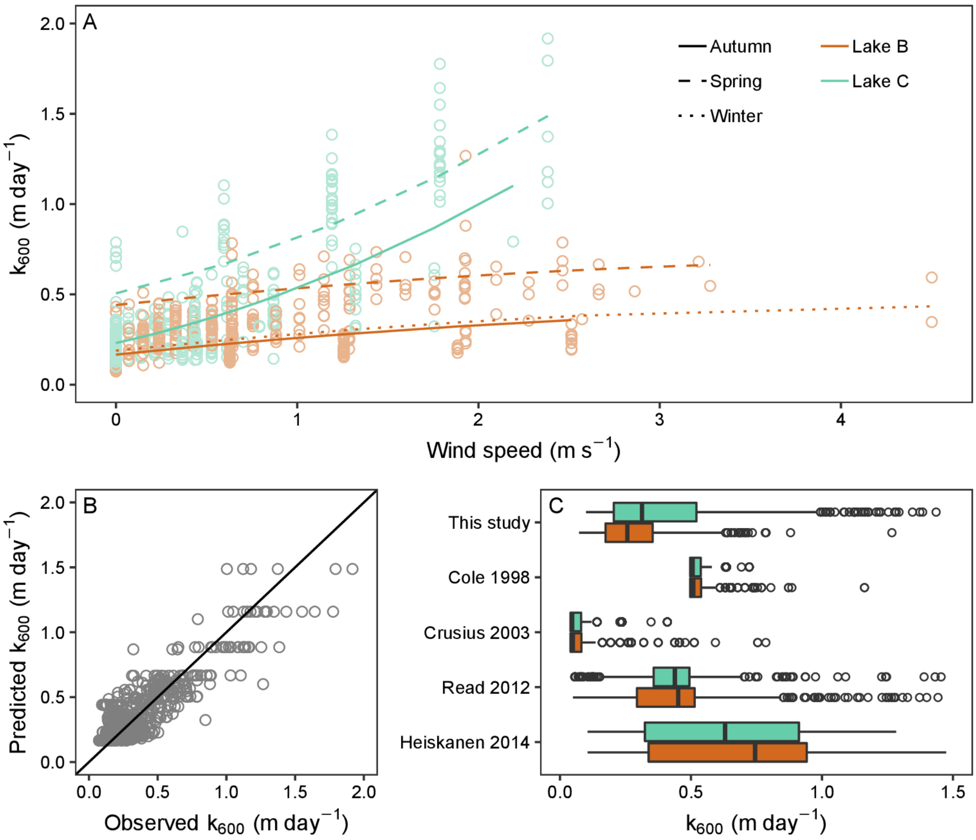

Fig. 5 Panel A. Relationship between k_{600} (y-axis) and wind speed (x-axis) colored by site (Lake B as brown and C as green). Points show measurements and lines show the fitted linear models by season.

Panel B. Predicted values from the fitted linear model plotted *versus* the observed values

Panel C. Box plots for each site comparing the observed k_{600} values (this study) to k_{600} values derived from four existing models of differing complexity. Box plots show median (solid horizontal line), 25% and 75% quartile (upper and lower hinge), vertical lines extend 1.5 times the inter-quartile range and observations outside this range are points

This is a post-peer-review, pre-copyedit version of an article published in Aquatic Sciences. The final authenticated version is available online at: https://doi.org/10.1007/s00027-019-0682-8

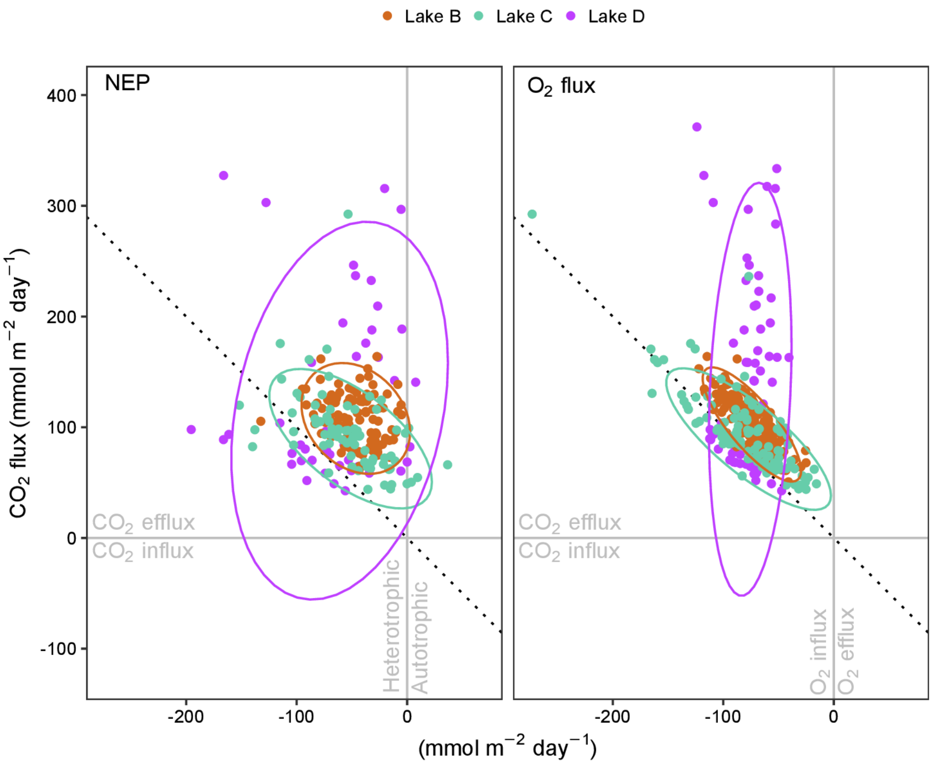

Fig. 6 CO_2 flux (y-axis) *versus* net ecosystem production, NEP (left, x-axis) and O_2 flux (right, x-axis), all units in mmol m^{-2} day^{-1}, colored by site. Points show observations superimposed by 95% confidence ellipses for each lake. The dotted line is the 1:1 line for which the CO_2 efflux matches the O_2 influx or the generation of CO_2 by NEP (assuming a respiratory quotient of 1)

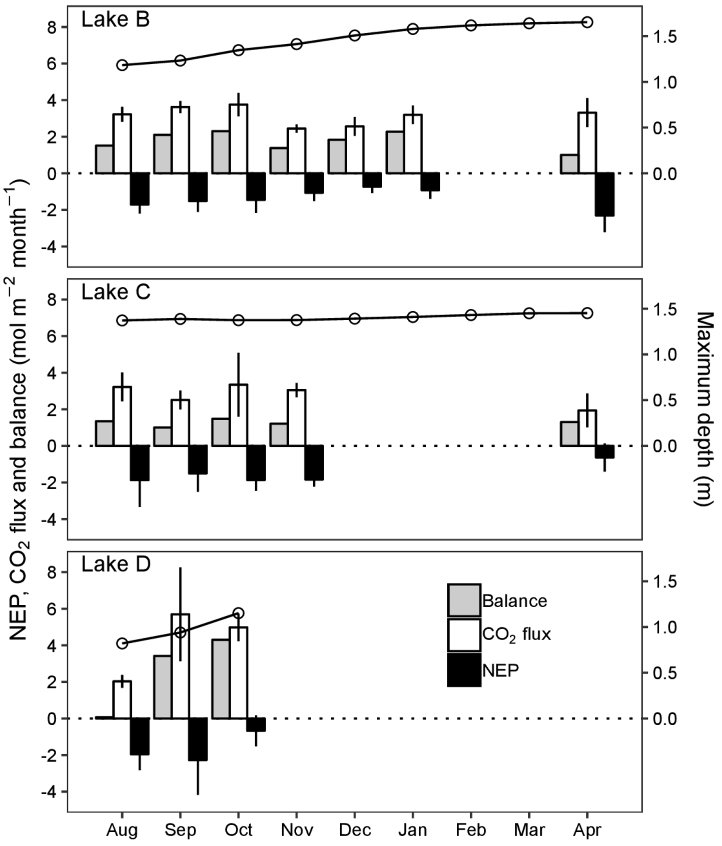

Fig. 7 Mean monthly values of net ecosystem production (NEP, black), CO_2 efflux (white) and balance (NEP-CO_2 efflux, grey) in Lakes B, C and D. Vertical lines are standard deviation. Monthly mean maximum depths (secondary y-axis) are connected by solid lines

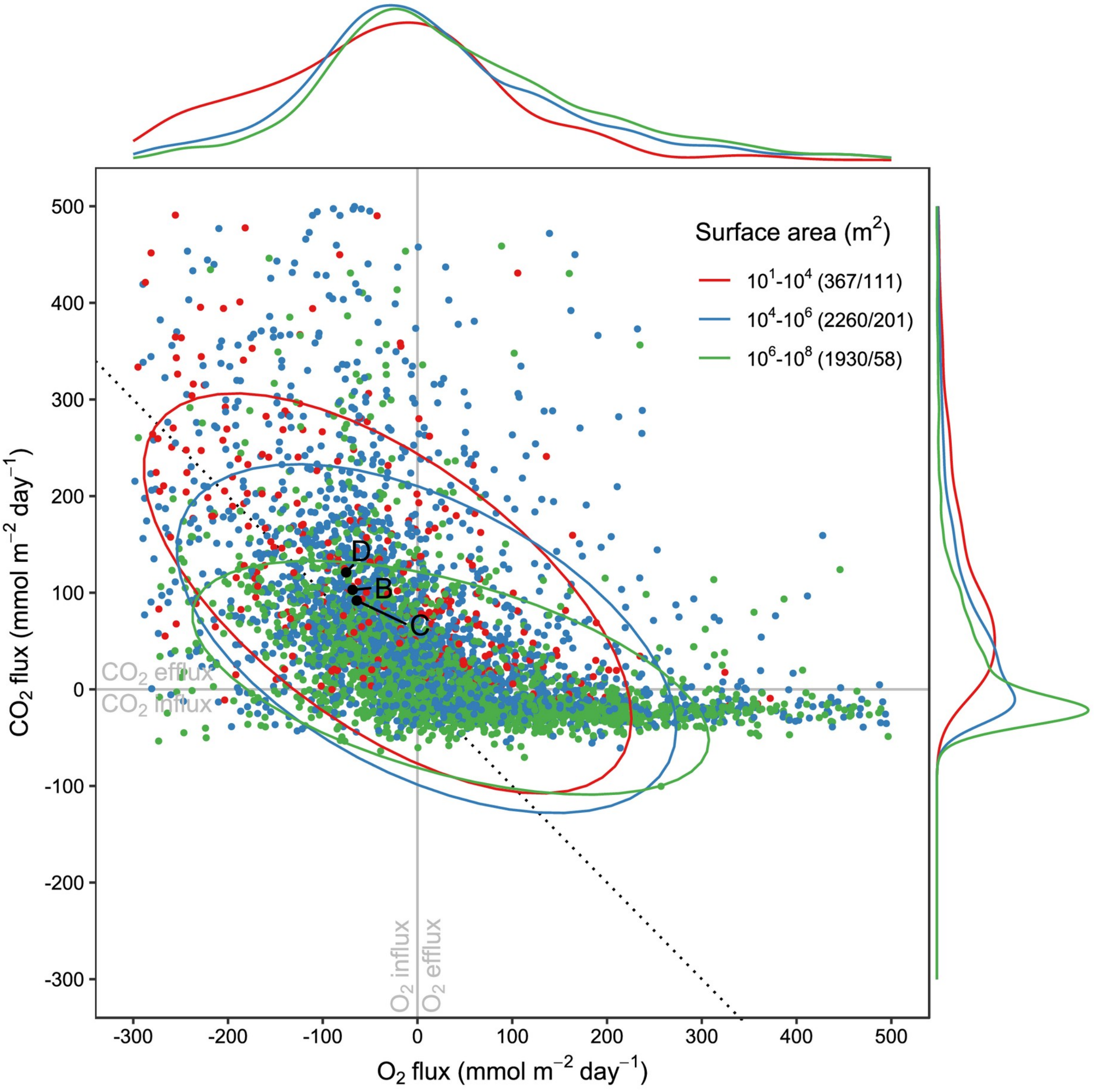

Fig. 8 CO_2 flux (y-axis, mmol m^{-2} day^{-1}) *versus* O_2 flux (x-axis, mmol m^{-2} day^{-1}) calculated from 4557 observations in 370 Danish lakes, which are colored according to three different surface area ranges (163 observations outside plotting range). Number of observations/number of sites are in the parenthesis in the legend. Points show observations superimposed by 95% confidence ellipses for each lake size range. Marginal plots show the density distributions for CO_2 flux (right) and O_2 flux (top). Mean values of the three lakes investigated in this study are also shown (B, C and D). The dotted 1:1 line shows similar CO_2 efflux and O_2 influx

Table 1 Size, chemical and optical characteristics of the investigated lakes over the year in Lake B and C and in September-October in Lake A and D. Values are reported as: mean (standard deviation, number of determinations)

Variables (unit)	Area (m^2)	Maximum depth (m)	Alkalinity (meq L^{-1})	pH	Light attenuation (m^{-1})	CDOM$_{440}$ (m^{-1})	*Chl a* (µg L^{-1})	Total-P (µg P L^{-1})	Total-N (µg N L^{-1})	Ortho-phosphate (µg P L^{-1})	Ammonium (µg N L^{-1})	Nitrate (µg N L^{-1})
Lake A	882 (±445, 10)	1.1 (±0.1, 10)	0.8 (±0.1, 9)	6 (±0.2, 10947)	9.7 (±5.5, 77)	17 (±1, 4)	23.9 (±37.6, 4)	331 (±30, 3)	2271 (±338, 3)	151 (±6, 3)	255 (±134, 3)	20 (±0, 3)
Lake B	6699 (±636, 20)	1.4 (±0.2, 20)	1.4 (±0.3, 23)	7.2 (±0.2, 40570)	3.8 (±1, 307)	11.1 (±2.1, 9)	10.9 (±8.1, 10)	156 (±51, 6)	2464 (±473, 6)	58 (±43, 6)	521 (±357, 6)	224 (±197, 6)
Lake C	4965 (±48, 21)	1.4 (±0.1, 21)	1.1 (±0.1, 23)	7.2 (±0.1, 17883)	5.7 (±3.4, 228)	7 (±1.4, 8)	19.6 (±24.5, 10)	140 (±47, 6)	1369 (±286, 6)	47 (±37, 6)	152 (±119, 6)	52 (±55, 6)
Lake D	369 (±77, 9)	1 (±0.1, 9)	3.4 (±0.5, 6)	7.6 (±0.2, 14206)	9.6 (±6.5, 35)	9.3 (±1.1, 4)	8 (±12.2, 4)	128 (±23, 3)	1808 (±306, 3)	25 (±16, 3)	207 (±115, 3)	70 (±50, 3)

Table 2 Water temperature, oxygen saturation, daily mean air-water gas fluxes (using pCO$_2$ estimated from pH and alkalinity) and daily metabolism of the investigated lakes over the year in Lake B and C and in September-October in Lake A and D. The intercept and the slope are estimated from the relationship R-GPP (model II regression, normalized to 20 °C). Values are reported as: mean (standard deviation, number of determinations)

Variables (unit)	Water Temperature (°C)	Dissolved oxygen (%)	CO$_2$ flux (mmol m^{-2} day^{-1})	O$_2$ flux (mmol m^{-2} day^{-1})	GPP (mmol m^{-2} day^{-1})	NEP (mmol m^{-2} day^{-1})	R (mmol m^{-2} day^{-1})	Intercept (mmol m^{-2} day^{-1})	Slope
Lake A	15.1 (±2.4, 14631)	15 (±14, 14631)							
Lake B	11.4 (±7.6, 48424)	59 (±28, 48424)	103 (±23, 158)	-67 (±29, 233)	63 (±67, 209)	-33 (±34, 209)	96 (±77, 209)	1.8 (1.4-2.2)	1.1 (1-1.2)
Lake C	10.2 (±7.1, 47424)	67 (±26, 47424)	96 (±38, 105)	-65 (±49, 226)	53 (±44, 176)	-38 (±36, 176)	91 (±51, 176)	2.4 (1.7-2.9)	1.2 (1.1-1.4)
Lake D	16.1 (±2.7, 13510)	42 (±19, 13510)	146 (±88, 63)	-76 (±18, 92)	64 (±65, 71)	-71 (±46, 71)	135 (±88, 71)	4.2 (3-5.1)	1.4 (1.2-1.6)